J. Ocean Univ. China (Oceanic and Coastal Sea Research)
https://doi.org/10.1007/s11802-020-4171-4
ISSN 1672-5182, 2020 19 (4): 790-800
http://www.ouc.edu.cn/xbywb/
E-mail:xbywb@ouc.edu.cn

Centurial Evolution of an Offshore Mud Deposition Area in the Changjiang (Yangtze) Estuary and Its Links to Environmental and Anthropogenic Activities

CONG Jingyi[1), 2)], HU Gang[2), 3), *], JONELL Tara N.[4)], YUAN Zhongpeng[1), 2)], KONG Xianghuai[2), 3)], ZHANG Yong[2), 3)], and WANG Yonghong[1)]

1) *College of Marine Geosciences*, *Ocean University of China*, *Qingdao* 266100, *China*
2) *Qingdao Institute of Marine Geology*, *China Geological Survey*, *Qingdao* 266071, *China*
3) *Laboratory for Marine Mineral Resources*, *Qingdao National Laboratory for Marine Science and Technology*, *Qingdao* 266071, *China*
4) *School of Earth and Environmental Sciences*, *the University of Queensland*, *St. Lucia* QLD 4072, *Australia*

(Received March 14, 2019; revised May 10, 2019; accepted October 23, 2019)

Abstract Large amounts of sediments originating from the Changjiang (Yangtze) River are deposited in the subaqueous delta and in the adjacent muddy area off the mouth and on the inner shelf of the East China Sea. The terrestrial sediments deposited in these areas not only contain information about the composition and environment of the source area, but they also record changes in anthropogenic activities. A sediment piston core (CJ0702) was extracted from the Changjiang subaqueous depocenter (31.00˚N, 122.67˚E) in a water depth of 22.0 m. The core was subsampled at 1–2 cm intervals and analyzed for grain size, clay mineralogy, and major element geochemistry. Results indicate a relatively high sediment accumulation rate of approximately 3.11 $cm\,yr^{-1}$. These parameters exhibited only minor cyclical fluctuations in the core, which resulted from many factors. During the past 120 years, the Changjiang River-derived sediment is the primary source of sediment in the offshore mud area without evidence for the Yellow River-derived sediment increasing. After the trunk stream shifted from the North Branch to South Branch, the variations of proxies are controlled by the periodic fluctuation possibly linked to El Niño-Southern Oscillation (ENSO) and the Pacific Decadal Oscillation (PDO). In addition, anthropogenic heavy metal concentrations can be divided into three stages, which coincide well with economic development and environmental protection policies.

Key words sedimentary evolution; mud area; Changjiang (Yangtze) Estuary; sediment transport; anthropogenic activity

1 Introduction

A river acts as a major land-ocean connection, discharging about 36000 km^3 of freshwater and 23 billion tons of suspended and dissolved solids to the coastal area (Milliman and Farnsworth, 2011). River deltas, which combine complex physical, chemical, biological, and geological processes, are major areas of energy and material exchange between land and ocean (Hori *et al*., 2001). The transport, accumulation, and preservation of this huge amount of river-derived material have formed sedimentary records, which can be used to reconstruct past climate, environments, and ecosystem changes (Gao and Collins, 2014). As they are covered by seawater, sediments deposited on the seafloor contain a relatively continuous sequence compared with those exposed to the atmosphere. The natural sediments found in coastal shelf areas (Stanley and Chen, 1993; Hori *et al*., 2002; Petley, 2010; Orpin *et al*., 2010; Gao, 2013), deep sea areas (Berger, 2013), ice (Davies *et al*., 2012), and coral reefs (Yu *et al*., 2006) contain indicators, which may be useful for paleoclimate or paleoenvironmental analysis. The coastal inner shelf has many advantages for studying environmental evolution based on the sedimentological record, especially during the Holocene, due to the vast quantities of terrestrial sediment transportation and subsequent high sedimentation rates.

Meanwhile, the Changjiang River is one of the five largest rivers in the world in terms of both sediment load and water discharge. It transports large amounts of terrestrial materials to the East China Sea (ECS) (Huang *et al*., 2001). The amount of annual sediment load discharged into estuaries and coastal and adjacent areas is estimated to be about 4.86×10^8 t (Milliman *et al*., 1985b). These near-shore regions can act as sinks of anthropogenic pollutants, and potentially cause environmental degradation and changes in the substrate environment (Gao and Wang, 2008; Hao *et al*., 2008). Recent studies from these centers storing se-

* Corresponding author. E-mail: hg_jinan@163.com

diment have allowed the reconstruction of the local sediment dynamics, sedimentary formation and evolution, past sea-level changes, sediment transport, and provenance into regional paleoenvironmental and paleoclimatic changes (Hori *et al*., 2001, 2002; Chen *et al*., 2003; Wang *et al*., 2005; Yang *et al*., 2007; Liu *et al*., 2010). In this fashion, the mud deposits from the Changjiang River in the ECS have recently become a research hotspot due to their high sedimentation rate and function of recording abundant information regarding sediment sources, climate change, and sedimentary evolution throughout the Holocene (Xiao *et al*., 2004, 2005; Liu *et al*., 2006, 2007; Qiao *et al*., 2011, 2017; Liu *et al*., 2013). Previous studies have mostly focused on the sedimentary evolution of this river system over geological timescales ($<10^6$ yr), and relatively few studies have investigated changes operating on shorter timescales (10^0-10^2 yr). Anthropogenic processes are very short relative to longer geologic timescales; however, as human society developed, an increasing number of studies have emphasized the importance and influence of these shorter timescale processes on even long-term evolutionary processes in river systems (Yang and Chen, 2007; Fan *et al*., 2011; Liu and Fan, 2011; Wang *et al*., 2012). Unfortunately, these studies have only focused on individual parameters in exploring the sedimentary evolution process of mud area during the past century. Hence, some related questions remain unanswered. Among them, the influential factors of grain size variation and sediment sources are still subject to ongoing debates.

Under the relative stable environment with no great changes on tectonic activity, sea-level change and oceanic hydrodynamics, the continuous high sedimentation rates of the Changjiang River allow the unparalleled opportunity to explore not only the offshore sedimentary evolution of the river system, but can also offer insights into the major factors influencing sedimentation, such as upstream internal basin dynamics, paleoclimatic change, and human activities. In particular, this study will explore the last 100 years at high resolution in muddy deposits sourced from the Changjiang River (Fig.1).

2 Regional Setting

The Changjiang subaqueous delta front is located in the ECS and is surrounded by the Yellow Sea, the Taiwan Strait, and the western Pacific Ocean. The ECS is located between the contiguous landmasses of Korea and China and forms a typical epicontinental shelf with strong tidal influences and complicated shelf circulation systems that exhibit characteristic seasonal and spatial variations (Lim *et al*., 2007). The ECS spans an area of 700000 km^2 and has an average water depth of 349 m, although the water is <200 m deep along most of the continental shelf.

Terrestrial sediments from the adjacent areas enter the ECS *via* many rivers, although the primary sediment sources are the Changjiang and Huanghe (Yellow) Rivers, whose sediment discharge exceeds 1.5×10^9 t annually (Milliman and Meade, 1983). The Changjiang River, already the third largest river in the world in terms of length and water discharge, has a length of 6300 km, making it the longest river in Asia. This river is globally renowned for its tremendous sediment and water discharges amounting to 4.68×10^8 t and 955×10^9 m^3 respectively. As a result, a large subaqueous, tidal-dominated delta has formed off the river mouth and covers an area of approximately 10000 km^2 (Liu *et al*., 2009b).

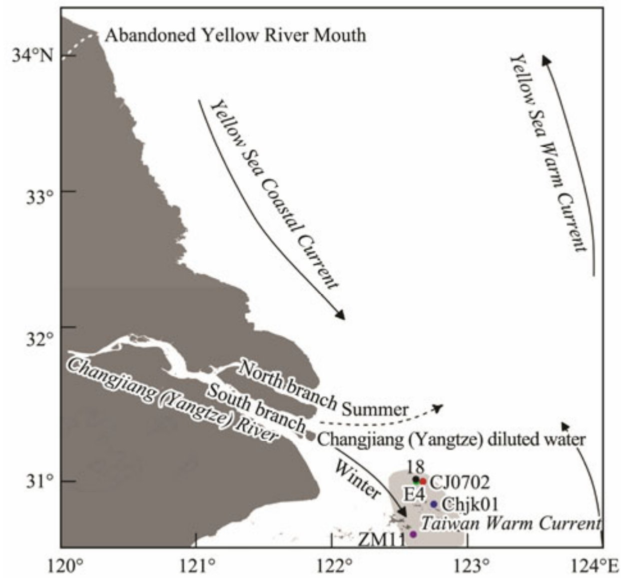

Fig.1 Sample locations and regional circulation patterns off the Changjiang River Mouth and adjacent areas (cores Chjk01, E4, ZM11, and 18 are from Yang and Chen, 2007; Liu and Fan, 2011 and Wang *et al*., 2012).

The Huanghe River, which originates on the Tibetan Plateau and flows across the dry Loess Plateau, also influences this area. The Huanghe is known for its large sediment load, which amounts to more than 1.0×10^9 t annually (Milliman and Meade, 1983). The Huanghe River shifted its course from the Bohai Sea to the southern Yellow Sea (SYS) between AD 1128 and 1855 (Yu *et al*., 1986). During this period, the river formed a large subaqueous delta on the western edge of the SYS, now named the abandoned Huanghe River Delta (Fig.1). As the Huanghe River has flowed into the Bohai Sea since AD 1855, the abandoned Huanghe River Delta has been eroded since then. At present, it is now an important sediment source for both the SYS and ECS. Sediments from the Huanghe and Changjiang Rivers are transported and distributed through the SYS and ECS, thus forming a unique distribution pattern. The region of interest in this study, the mud area in the ECS, is a typical sedimentary deposit accumulated over the past 7000 years. Prior works have concluded that the Changjiang River is the primary source of sediment in this region (Liu *et al*., 2007; Xiao *et al*., 2009). Nevertheless, numerous offshore oceanographic and tidal processes also influence the transport and redistribution of Changjiang River sediment from the river plume across the SYS and ECS. The river plume, known as the Changjiang diluted water (CDW; Fig.1), can extend for hundreds of kilometers from the river mouth, reaching as far as Cheju Island in the summer. The river plume dispersal takes different routes depending on the season, with northeastward flows in summer and southward flows in winter. Continental coastal currents, including the North Jiangsu Coastal Current and the Yellow Sea Coastal Current (YSCC), commonly interact with the plume as they flow constantly southward along the western edge of the SYS and bring other sediments into the SYS and ECS.

3 Materials and Methods

One piston core (CJ0702), 375 cm-long, was extracted from the subaqueous depocenter (31.00˚N, 122.67˚E) in a water depth of 22.0 m by drilling vessel *Kan407* in May 2007. The exact location was approximately 90 km southeast of the present Changjiang River Mouth. The borehole site was at the periphery of the mud area (Fig.1). Once transported to the Qingdao Institute of Marine Geology Laboratory, the core was split, described, and subsampled. The entire core was divided into subsamples (approximately 1–2 cm-thick) for high-resolution analysis. In total, the core was divided into 240 subsamples from the top to the bottom. Subsamples were analyzed for grain size, ^{210}Pb dating, clay mineral assemblage, and element geochemistry. To obtain the age of sediments and determine the sediment accumulation rates, the ^{210}Pb dating of sediments was performed on the top 150 cm of the core. Forty fluvial sediments were collected from the Yellow River and Changjiang River in 2015 to be tested for clay mineral assemblage.

Next, to prepare the subsamples for grain size analysis, sediments were pretreated with 10% H_2O_2 and 0.1 mol L^{-1} HCl to remove organic matter and biogenic carbonate, respectively. The subsamples were analyzed with a Mastersizer 2000 laser particle size analyzer. The measurement range was between 0.02 and 2000 μm, with a resolution of 0.01 Φ and reproducibility better than 3%.

Core CJ0702 was taken from a sediment depocenter with notably high accumulation rates (DeMaster *et al.*, 1985; Yang and Chen, 2007). In this study, we calculate the accumulation rate by the method of constant initial concentration for ^{210}Pb, short-lived radioisotope with a half-life of 22.3 years and a decay constant of 0.031 yr^{-1} (Hohndorf, 1969). Dating sediments ^{210}Pb is considered reliable and is widely distributed in the estuaries and inner shelf areas (Yang and Chen, 2007; Fan *et al.*, 2011; Liu and Fan, 2011; Hulse and Bentley, 2012; Wang *et al.*, 2012). To date the core, 31 subsamples were selected at intervals of between 2 and 10 cm in the core for the ^{210}Pb, ^{226}Ra, and ^{137}Cs analysis in order to constrain the sediment accumulation rates. ^{210}Pb activities were determined using a BE3830 gamma-ray spectrometer (Canberra Ltd., USA) at the Experiment Testing Center of the Qingdao Institute of Marine Geology.

Additionally, the resulting products for the atmospheric and terrestrial sources of ^{210}Pb are referred to as supported ^{210}Pb and excess $^{210}Pb_{ex}$ (Goldberg, 1963). Constraining the $^{210}Pb_{ex}$ activities can be used to calculate the accumulation rate of sediments over the centennial timescales.

All samples were analyzed for major element geochemistry at the Experiment and Testing Center of Qingdao Institute of Marine Geology, China Geological Survey. Major and trace elements (Si, Al, Ca, Mg, Na, total Fe, K, Ti, P, Cu, Zn, Ga, Rb, Sr, Zr, Nb, Cs, Ba, Hf, and Pb) were determined by X-ray fluorescence using a Phillips PW 2440 spectrometer. The samples were prepared into fused glass disks following the method described by Xia *et al*. (2008). The concentrations of trace and rare earth elements were determined using the method described by Liu *et al*. (2009a).

Clay mineral analysis on <2 μm fraction was conducted at the Institute of Oceanology, Chinese Academy of Sciences. The grains were separated following Stoke's settling velocity principle after carbonate and organic matter were removed by treatment with 15% hydrogen peroxide and acetic acid (25%), respectively. Clays were fully dispersed by an ultrasonic cleaner, dried at room temperature, and smeared on glass slides for analysis. Clay mineral analysis was conducted using X-ray diffraction with a D8 ADVANCE diffractometer with CuKa (alpha) radiation (40 kV, 40 mA) at the Institute of Oceanology, Chinese Academy of Sciences. Clay mineral fractions were identified and calculated using the described methods of Thamban *et al*. (2001) and Biscaye (1965).

4 Results

4.1 ^{210}Pb Chronology and Lithology

Core CJ0702 is generally uniform in color and sediment fraction, and is dominantly made up of silt and clay with minor sand. The core, from top to bottom, consisted of yellowish-brown clayey silt with intercalated dark gray silty laminae and some wormholes. There were abundant intercalations of clayey silt and silt, with 1–3 mm-thick silt interbeds in the lower section. The bottom section was composed of dark gray clayey silt with lenses or laminations of silt or occasional fine sand (referring to Hu, 2014).

Profiles of excess $^{210}Pb_{ex}$ revealed a mean sediment accumulation rate of 3.11 cm yr^{-1}. The top section of homogeneous $^{210}Pb_{ex}$ and the bioturbated fabrics indicated a mixed layer thickness of 10 cm. Below the mixing layer, the excess $^{210}Pb_{ex}$ concentrations decreased steadily from the mixing layer to a depth of 120 cm (Fig.2) and then maintained a constant value below 120 cm. Therefore, a mean accumulation rate of 3.11 cm yr^{-1} was calculated from the ^{210}Pb data (standard deviation of r^2 = 0.56). This result is consistent with the previous results collected from the same area (Yang and Chen, 2007; Fan *et al*., 2011; Liu and Fan, 2011; Wang *et al*., 2012). Based on this accumulation rate, core CJ0702 spans roughly 120 yr, from approximately 1887 to 2007 along its 375 cm length.

The core represents only the past 120 years; thus, geologic factors, which allow us to ignore sediment compaction effects, tectonic uplift or subsidence, and sea-level changes, will not be significant in its interpretation. In addition, there were no substantial changes to either ocean circulation in this area nor in the large-scale sediment transport patterns over this short timescale. The data show periodic fluctuations in grain size, clay mineralogy, and geochemistry (Figs.3–6), suggesting that these variations result from many factors, such as provenance, weathering, and local hydrodynamics. There were only modest variations in the relatively high accumulation rate (3.11 cm yr^{-1}).

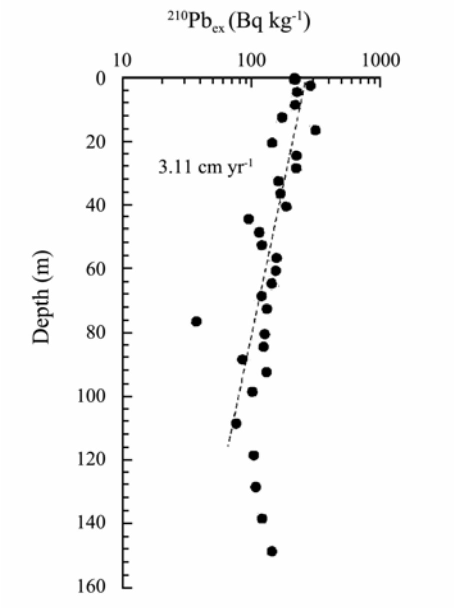

Fig.2 $^{210}Pb_{ex}$ concentration profiles and accumulation rate for core CJ0702.

4.2 Variations in Grain Size

Grain size fluctuated periodically for the whole length of the core (Fig.3). The mean grain size ranged from 5.58–7.66Φ, with an average of 7.13Φ. These values generally correspond to those of deposition within muddy systems. The clay content ranged from 13% to 39%, with an average of 30%. The silt content ranged from 56%–78%, with an average of 68%. The core contains a small amount of sand, ranging from 0–24%, with an average of 2%. The standard deviation, or sorting coefficient, ranged from 1.32 to 2.17, with an average of 1.59, indicating relatively poor sorting. The skewness ranged from −0.40 to 0.76 (average = 0.08) and had a mostly symmetrical distribution.

The core CJ0702 can be divided in to three sections according to grain size variation (Fig.3). The bottom section (from 1887 to 1903) shows that the mean grain size increases gradually as the skewness becomes greater, indicating the coarsening of the sediment. The sorting coefficient increased gradually from the bottom of the core, through the middle section, and into the upper section of the core. The middle section (from 1903 to 1980) demonstrates that the mean grain size is greater than the bottom section and has relatively modest variation. In addition, the skewness was much greater than the bottom section. This suggests that the sediment becomes coarser, thus matching the grain size variation. The top section (from 1980 to 2007) illustrates greater fluctuation ranges in terms of grain size, sorting coefficient, and skewness. These variations displayed relatively complex dynamics.

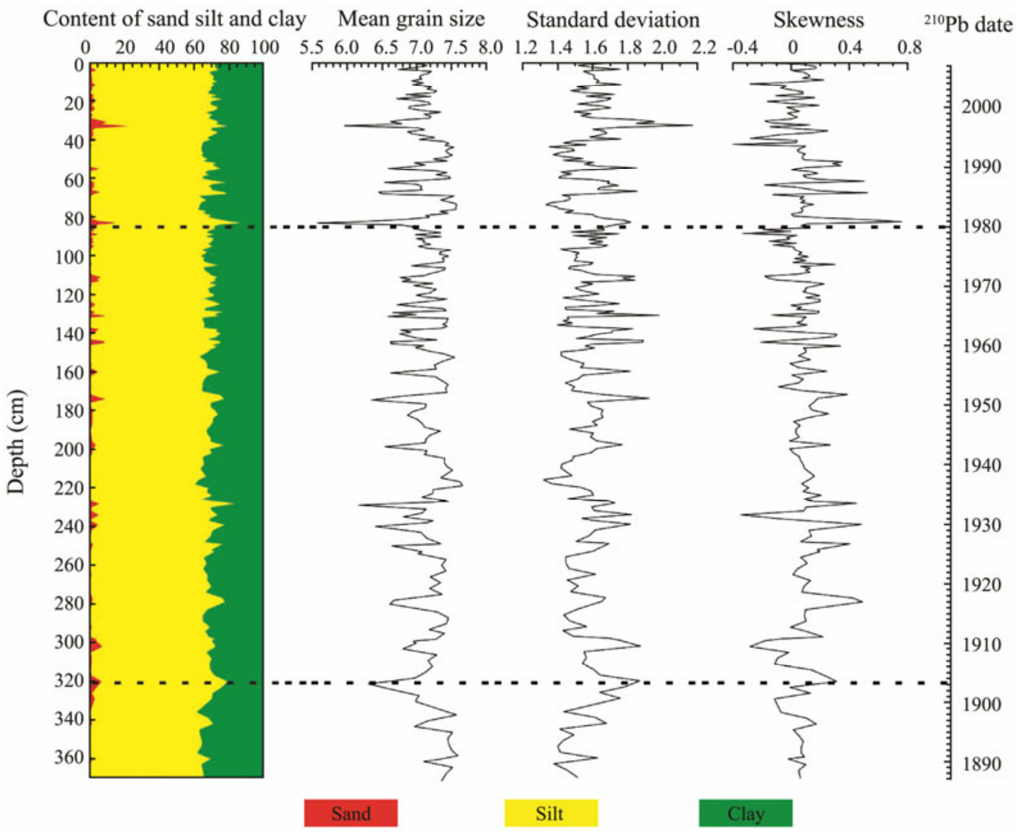

Fig.3 Distribution of the grain size parameters in core CJ0702 (modified after Hu, 2014).

4.3 Clay Mineralogy

The dominant clay mineral in Core CJ0702 was illite whose content ranged from 55%–75%, with an average of 65%. The chlorite content was the next highest, ranging from 9% to 18%, with an average of 14%. Smectite and kaolinite contents ranged from 2% to 22% and 4% to 16%, respectively. Their average contents were 11% and 10%, respectively (Fig.4).

There were no clear variations in the contents of the four quantifiable clay minerals in core CJ0702. This finding shows a relative stable source, but the greatest variation is observed at the top. However, quantitatively distinguishing the proportions of Changjiang River and Huanghe River sediment sources in this core proved to be difficult by using the mineralogical method evidenced by Fan *et al*. (2001).

4.4 Distributions of Major and Trace Elements

Sediment SiO_2 contents ranged from 51%–63%. The average contents of Fe_2O_3, CaO, MgO, and K_2O varied between 3.13% and 6.54%. The concentrations of the other major elements were very small. The coefficients of variation of the major elements varied between 0.01 and 1.84, with an average of 0.38. These measurements indicated that there was little fluctuation in the major element contents throughout the core. Fe, Mg, K, Ti, and Mn were mainly of terrestrial origin and were thus positively correlated with Al, with correlation coefficients higher than 0.77. As the chemical elements in the sediment were strongly influenced by sediment grain size (Zhao and Yan, 1994), we removed this effect by normalizing the elements with Al_2O_3 (Fig.5).

Five distinct phases were observed in core CJ0702. 1)

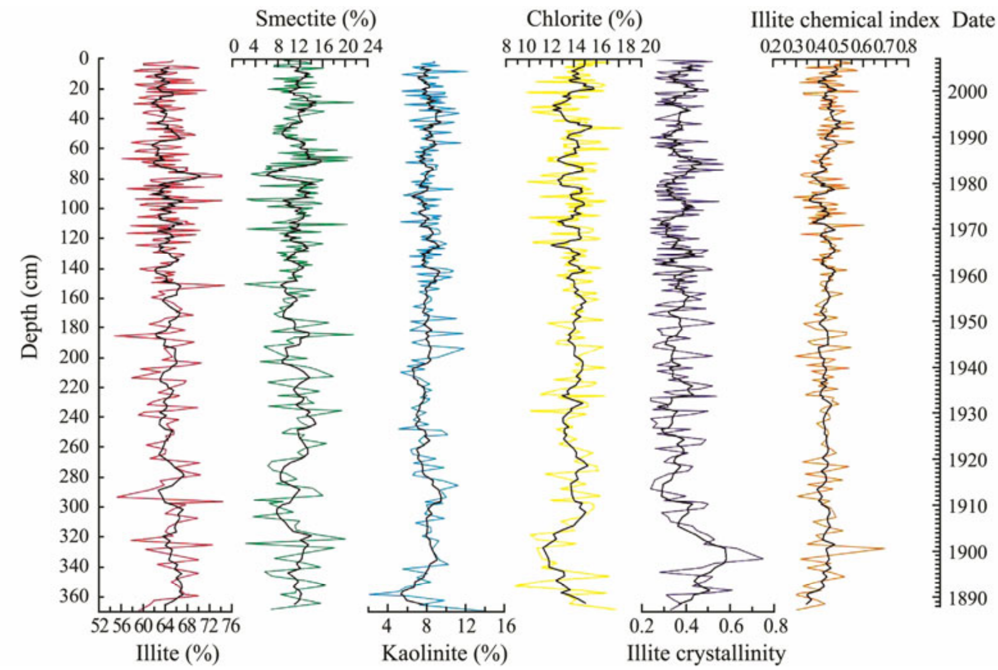

Fig.4 Downcore variations in clay mineralogy in core CJ0702. Black lines represent a five-point moving average for each clay mineral.

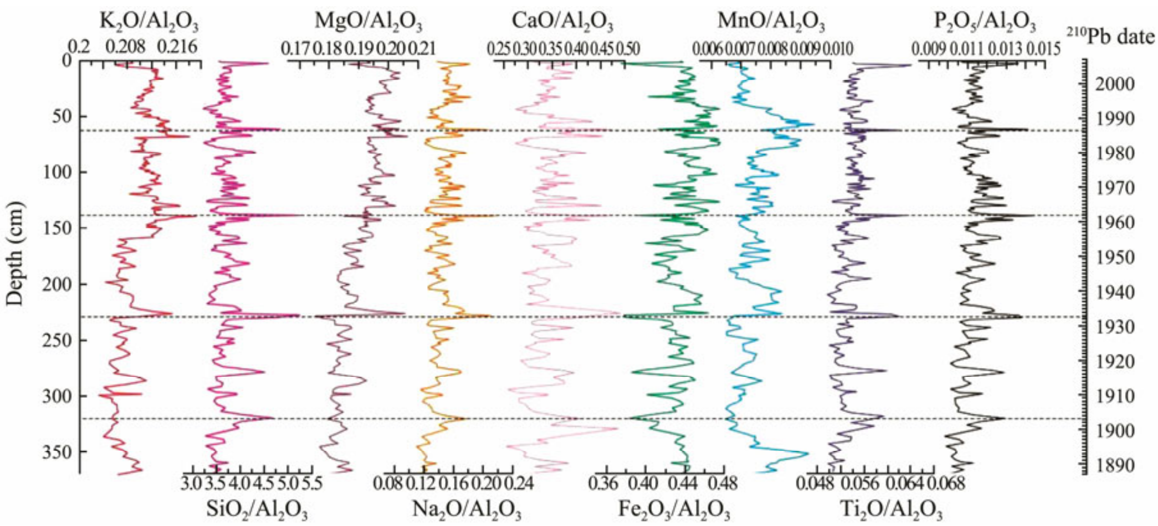

Fig.5 Downcore variations of the major elements in core CJ0702.

From the bottom of the core at 375–320 cm, the contents of SiO_2, Na_2O, CaO, Ti_2O, and P_2O_5 were lower than the upper sections and increased upward, whereas Fe_2O_3, MgO, K_2O, and MnO were in the opposite trends, which were higher than the upper sections in contents and decreased upsection. 2) From 320–230 cm, there were fluctuation variations and three value peaks found in all elements curves. The Fe_2O_3 and MnO showed an opposite distribution trend with other elements in this section. 3) Between 230 and 145 cm, the contents of all elements exhibited small periodic changes and low fluctuation, and most of the major elements displayed an increasing trend in this section. 4) Between 145 and 60 cm, there were greater fluctuations in the contents of the major elements compared to the underlying interval and a very weak periodicity. In addition, most of the major elements showed an increasing trend. 5) From 60 cm to the top of the core, elemental concentrations were relatively stable, except the elements Fe_2O_3, K_2O and MnO which have a sharp decrease.

There were no notable coherent trends in the downcore distribution of trace element concentrations except the heavy metals Pb, Hg, and Zn (Fig.6). Trace element abundances can be divided into four categories: those with concentrations greater than 1000 $\mu g\,g^{-1}$ (Cl); those with concentrations greater than 100 $\mu g\,g^{-1}$ (S, Zn, Sr, Zr, Ba, Rb); those with concentrations greater than 1 $\mu g\,g^{-1}$ (Cu, Pb, As), and those with concentrations lower than 1 $\mu g\,g^{-1}$ (Cd, Hg). The coefficients of variation of Cl, S, and P and some heavy metals were all greater than 12%, indicating a certain degree of dispersion and relatively large changes.

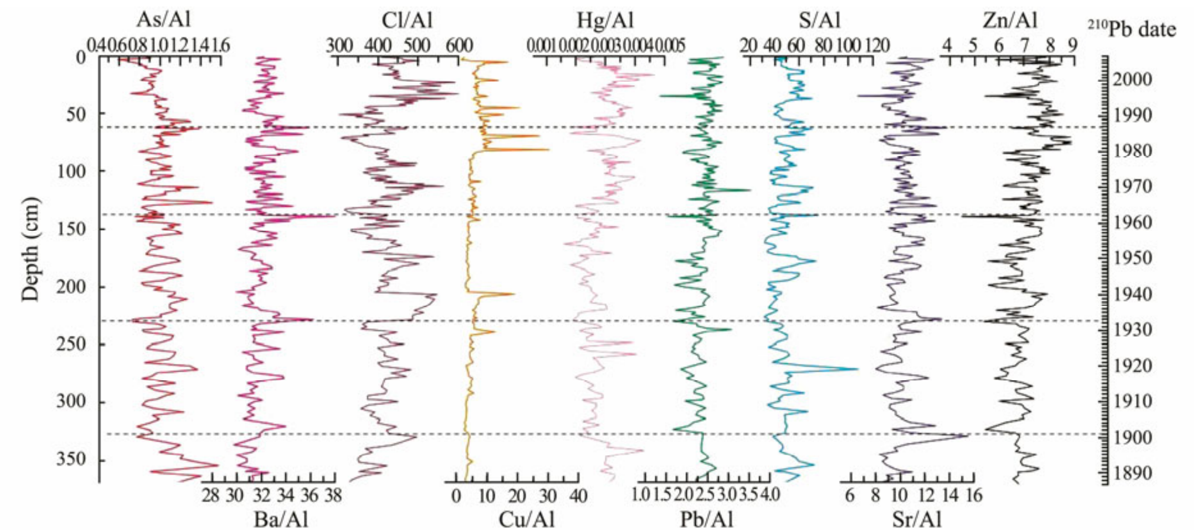

Fig.6 Downcore variations of the heavy elements in core CJ0702.

5 Discussion

5.1 Sediment Source of the Muddy Area

Mud deposition offshore the Changjiang River Mouth began in the mid-Holocene when the modern current circulation patterns developed in the ECS (Liu *et al*., 1999; Li *et al*., 2007; Xiang *et al*., 2008). Since that time, sediments from the Huanghe and Changjiang Rivers have been considered the main sources of sediments to the ECS. It is likely the muddy area is primarily sourced from the Changjiang River-derived sediment, but is also influenced by the Huanghe-derived sediment (Liu *et al*., 2010; Hu *et al*., 2014). Based on the calcite variation, which has been used as indicator of the Huanghe River provenance in sediments (Milliman *et al*., 1985a), the sediment flux from the Huanghe River to the research area has intensively increased during the last 600 years (Liu *et al*., 2010). This conclusion, however, is the subject of ongoing debates and should be further considered with more precise dating and proxies.

Our data show no obvious change in smectite content, which indicates a relatively stable source in the core (Fig.4). Clay minerals indicate dominant sourcing from the Changjiang River (Fig.7). First, as a result of the Huanghe River changing its course from the Bohai Sea to the SYS between AD 1128 and 1855, the amount of sediment discharge resulted in the progradation of a large subaqueous delta, now named the 'abandoned Huanghe River Delta', along the western SYS. The shoreline near the abandoned Huanghe River Mouth has rapidly moved eastward by about 90 km at a rate of 100 $m\,yr^{-1}$ (Zhang, 1984; Ye, 1986; Li, 1991). According to Pang *et al*. (2016), most of the sediments are accumulated in the abandoned Huanghe River Delta. The resuspended sediment from the abandoned delta is transported southeastward and interface with the Yellow Sea Warm Current (YSWC) to generate the southwestern Cheju Island mud. This means that the majority of the sediments are discharged into the SYS to form the subaqueous delta and adjacent area while lower amounts of sediments are transported to the farther ECS. After the abandonment of the Huanghe River Delta at AD 1855, the Huanghe River has gradually eroded and transported the delta sediments to the SYS and ECS. Following the avulsion of the lower reaches after the reduction in sediment supply, the shoreline near the abandoned Huanghe River Delta has receded by more than 20 km during the past 150 years (Liu *et al*., 2010). This phenomenon indicates that vast amounts of eroded sediments, approximately 5×10^8 t yr^{-1} (Hu *et al*., 1998), should be transported by longshore currents to the ECS and should be a likely source to the samples analyzed in this study. This is in contrast to the lack of variation in sediment source, as suggested by clay mineralogy (Figs.4 and 7).

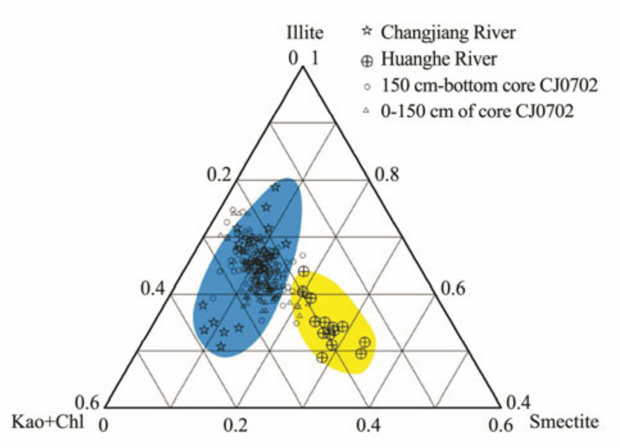

Fig.7 Ternary plot of the clay minerals in core CJ0702. Sediments derived from the Changjiang River and Huanghe River are presented in the blue area and yellow area, respectively.

Second, the Changjiang River-derived sediment demonstrates various patterns in different season. The CDW flows eastward and northeastward to interact with the Taiwan Warm Current in summer. This current then transports some amount of Changjiang River-derived sediments that are deposited at the offshore area of the Changjiang River Mouth. The CDW flows southward with the extensive YSCC in winter. This strong longshore current results in a high concentration of resuspended sediment in the west Yellow Sea and in the Changjiang offshore area. The resuspended sediments originating from the abandoned Huanghe River Mouth are transported southeastward along the Changjiang Bank and interface with the YSWC, eventually generating the southwestern Cheju Island mud (Sun *et al*., 2000; Pang *et al*., 2016). The Changjiang River-derived sediments that are deposited onto the offshore area are resuspended and transported by the CDW southeastward, thus contributing to the mud deposition.

With these relatively stable current circulations, we infer that the sedimentary dynamics is stable with a fixed sediment transport. Only a small amount of Huanghe River-derived sediments are deposited in the mud area off the Changjiang River Mouth. All the proxies, including the grain size (Fig.3), clay mineral assemblage (Fig.4), chemical element (Figs.5 and 6) present a relatively stable environment which suggest a stable source of Changjiang River during the past 120 years.

5.2 Influential Factors in Grain Size Variation

Although sediment source terranes can strongly influence grain size variation, we suggest that hydrodynamic factors, such as currents, runoff, and wave action, played a primary role in grain size variability observed in the current work. Previous studies have revealed some factors that influence the variation of grain size in the same study area within sediment cores Chjk01, E4, 18, and ZM11 (Fig.1; Yang and Chen, 2007; Liu and Fan, 2011; Wang *et al*., 2012). It has been proposed that the most important factor resulting in grain size variation is a branch shift of the Changjiang trunk stream into the sea. This shift results in a variable distance between the sampling station and the location of the Changjiang trunk stream into the sea. In addition, there is no relationship between the variation of water and sediment discharge and the Asian monsoon index. The down-core distribution of grain size indicates small fluctuations without sharp grain size changes, thus suggesting a relatively stable depositional environment without extreme changes. This is supported by the lack of fundamental changes in the source terrane. Therefore, we suggest that the sedimentation processes are mainly controlled by the hydrodynamic changes resulting from the periodic climate change and event-related processes.

There is an increasing trend of grain size before 1900 according the grain size distribution in Fig.3. The Changjiang River trunk stream to the sea shifted from the North Branch to the South Branch after the 1870s, which resulted in a smaller distance between our research site and the trunk stream (Yang and Chen, 2007). During the next 20 years, the trunk stream shifted in the south branch while the distance with sampling station varied slightly. Therefore, the sediment grain size becomes coarser from the bottom to 1900 with the adaptation to the new environment (Fig.3).

Within the middle section of the core (Fig.3), we suggest that there is a shift in the dominant control on grain size. Previous grain size variations can be attributed to branch shifting, this part of the section indicates control by local climate cycles, such as the Pacific Decadal Oscillation (PDO) and the El Niño-Southern Oscillation (ENSO). The PDO has caused decade-scale climate change in the northern Pacific, whereas ENSO often causes inter-annual variations in sea surface temperatures in the tropical Pacific. These two factors lead to variations in precipitation across China, resulting in changes in annual to decadal fluvial sediment and water discharges (Huang and Wu, 1989; Wang and Gong, 1999; Yang *et al*., 2004; Zhou *et al*., 2009; Liu *et al*., 2010; Ren *et al*., 2012).

The wavelet analysis of the Chemical Index of Alteration (CIA) indicates that the CIA has a consistent cycle, similar to the 2- to 8-year periodicities of ENSO (Fig.8). In addition, the higher CIA values match with the ENSO and PDO events consistently (Fig.8). The variations in CIA (McLennan, 1993) are due to the periodical variations in sediment and water discharges caused by extreme events, with corresponding changes in grain size. Therefore, the periodical climate change is the dominant factor determining the parameter variations of the middle section in the core.

In terms of the top section (from 1980 to 2007), greater fluctuation ranges are found in terms of grain size, sorting coefficient, and skewness. These variations display relatively turbulent dynamics. We propose that the major human projects, including the Three Gorges Dam, Estuarine Deepwater Channel, and flood water (*e.g.*, 1998 flood water) may have contributed to this variability. However, we cannot accurately define which is the strongest control in this study; thus, we recommend that further research on this topic should be conducted.

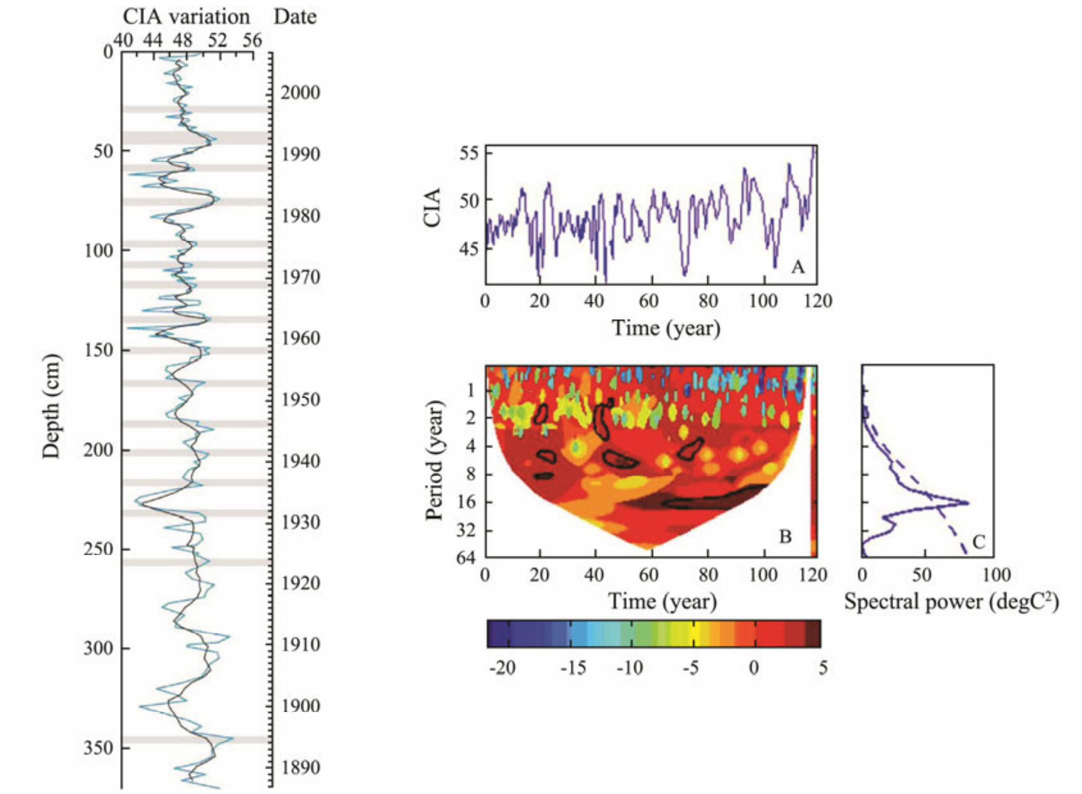

Fig.8 Downcore distribution of the CIA (Left) and responses to ENSO and PDO (Right): A) Variation of CIA with time; B) Wavelet analysis of CIA; C) Global wavelet spectral. The black line represents five points average line and the columns represent the date of PDO and ENSO referenced from Wang and Gong (1999).

5.3 Response of Sedimentary Processes to Anthropogenic Activities

Since the onset of the Industrial Revolution (1760s), natural resources have been discovered and increasingly exploited. The extraction, transport, and refinement of these resources by humans have resulted in significant environmental changes. As a result, the levels of anthropogenically sourced heavy metals in the environment have increased dramatically (Thevenon *et al*., 2011) and this contamination has become an essential indicator of environmental health (Chen *et al*., 2014). The Changjiang River basin, particularly the Changjiang Delta, is one of the most developed areas in China. As a result, large amounts of anthropogenic heavy metals have been delivered into the Changjiang River and deposited onto the subaqueous delta and adjacent mud area of the ECS (Lin *et al*., 2002). Correlation analysis shows that the Pb, Hg, As, and S concentrations reflect these anthropogenic contributions to sediments (Liu and Fan, 2011).

Similarly, heavy metals have been used as proxies for human activities in Core CJ0702, which we discuss as part of three discrete stages (Fig.6) detailed below.

Stage 1 (before 1950): China had a long history as an agrarian society and had a low level of industrialization until the 1950s. However, even during this stage, the Industrial Revolution had been underway for more than 100 years. Furthermore, the Changjiang River basin was involved in the World War II and China's War of Liberation between 1931 and 1949. The economic status of this area was poorly developed, and the heavy metal contamination by human activities was limited and maintained at a lower level than seen today (Lin *et al*., 2002; Fig.6).

Stage 2 (1950 – 1990s): After the founding of the so-called 'New China', agriculture and industry rapidly developed, leading to the increased use of the Changjiang River basin as an integral waterway. The discharge of polluted materials increased rapidly, corresponding to an increase in heavy metal contamination in the core (Fig.6). The section between 60 cm and 100 cm represents the 1980s. During this period, China reformed and adopted an open-door policy, which instigated the rapid development of the economy. Subsequent, extensive changes in the environment and increased quantities of heavy metals delivered offshore are clearly visible in the core.

Stage 3 (1990s – present): From the 1990s to the present day, a series of environmental protection policies have been implemented. Concentrations of Hg, As, S, and Pb in core CJ0702 gradually decreased from the middle of the 1990s (at a depth of 35 cm) (Fig.6). Thus, the influx of polluted materials, such as heavy metals, through the

Changjiang River Basin, subaqueous delta, and adjacent mud area has been controlled.

5 Conclusions

In this study, we established a high-resolution record of sedimentary processes near the Changjiang River Mouth from core CJ0702 in the subaqueous delta in the ECS. Core CJ0702 contains information about key environmental and human activities over the past 120 years. We observe a high sediment accumulation rate of 3.11 $cm\,yr^{-1}$ and relatively stable sedimentary processes during the past century. Though the course of the Huanghe River shifted to the Bohai Sea after 1855, the large subaqueous delta of the abandoned Huanghe River has been gradually eroded and transported to the Yellow and East China Seas. Thus, the Changjiang River has been the primary source of sediment to the core site.

Results suggest that the PDO and ENSO are vital factors that influence the sedimentary processes and are responsible for producing cycles in grain size variation. Event deposition, such as flood, storm, and human projects, also likely contributed to the sedimentary sequence in addition to climatic-drive grain size cycling. Indeed, human activities have had a great impact on the sediment composition, such that heavy metals in the core are closely correlated with anthropogenic activities tied to the industrial growth in this area.

Acknowledgements

This study was jointly funded by the National Natural Science Foundation of China (Nos. 41676052 and 41206 073), the State Scholarship Fund sponsored by China Scholarship Council (No. 201609370007), and the China Geological Survey (Nos. DD20190236, DD20160137, and DD20190205). We are grateful to those who took part in sampling, testing and photography, including Mr. Hongbo Ren and Mr. Zhigang Zhu from the Qingdao Institute of Marine Geology, and Drs. Jiaze Wang, Xufeng Zheng, and Jiang Dong from the Institute of Oceanology, Chinese Academy of Sciences, China.

References

Berger, W. H., 2013. Milankovitch tuning of deep-sea records: Implications for maximum rates of change of sea level. *Global Planet Change*, **101**: 131-143.

Biscaye, P. E., 1965. Mineralogy and sedimentation of recent deep-sea clay in the Atlantic Ocean and adjacent seas and oceans. *Geological Society of America Bulletin*, **76**: 803-832.

Chen, B., Fan, D. J., Li, W. R., Wang, L., Zhang, X. L., Liu, M., and Guo, Z. G., 2014. Enrichment of heavy metals in the inner shelf mud of the East China Sea and its indication of human activity. *Continental Shelf Research*, **90**: 163-169.

Chen, Z., Saito, Y., Hori, K., Zhao, Y., and Kitamura, A., 2003. Early Holocene mud-ridge formation in the Yangtze offshore, China: A tidal-controlled estuarine pattern and sea-level implications. *Marine Geology*, **198** (3-4): 245-257.

Davies, B. J., Hambrey, M. J., Smellie, J. L., Carrivick, J. L., and Glasser, N. F., 2012. Antarctic Peninsula ice sheet evolution during the Cenozoic era. *Quaternary Science Review*, **31**: 30-66.

DeMaster, D. J., McKee, B. A., Nittrouer, C. A., Qian, J. C., and Cheng, G. D., 1985. Rates of sediment accumulation and particle reworking based on radiochemical measurements from continental shelf deposits in the East China Sea. *Continental Shelf Research*, **4**: 143-158.

Fan, D. J., Qi, H. Y., Sun, X. X., Liu, Y., and Yang, Z. S., 2011. Annual lamination and its sedimentary implications in the Yangtze River Delta inferred from high-resolution biogenic silica and sensitive grain-size records. *Continental Shelf Research*, **31**: 129-137.

Fan, D. J., Yang, Z. S., Mao, D., and Guo, Z. G., 2001. Clay minerals and geochemistry of the sediments from the Yangtze and Yellow Rivers. *Marine Geology & Quaternary Geology*, **21** (4): 7-12 (in Chinese with English abstract).

Gao, S., 2013. Holocene shelf-coastal sedimentary systems associated with the Changjiang River: An overview. *Acta Oceanolgia Sinica*, **32** (12): 4-12.

Gao, S., and Collins, M. B., 2014. Holocene sedimentary systems on continental shelves. *Marine Geology*, **352**: 268-294.

Gao, S., and Wang, Y. P., 2008. Changes in material fluxes from the Changjiang River and their implications on the adjoining continental shelf ecosystem. *Continental Shelf Research*, **28**: 1490-1500.

Goldberg, E. D., 1963. Geochronology with ^{210}Pb: Radioactive dating. *Conference Proceedings, November 19-23, 1962, Athens*. Vienna, 121-131.

Hao, Y. C., Guo, Z. G., Yang, Z. S., Fan, D. J., Fang, M., and Li, X. D., 2008. Tracking historical lead pollution in the coastal area adjacent to the Yangtze River Estuary using lead isotopic compositions. *Environmental Pollution*, **156**: 1325-1331.

Hohndorf, A., 1969. Bestimmung der Halbwertszeit von ^{210}Pb. *Zeitschrift für Naturforschung*, **24A**: 612-615.

Hori, K., Saito, Y., Zhao, Q. H., Cheng, X. R., Wang, P. X., Sato, Y., and Li, C. X., 2001. Sedimentary facies and Holocene progradation rates of the Changjiang (Yangtze) Delta, China. *Geomorphology*, **41**: 233-248.

Hori, K., Saito, Y., Zhao, Q. H., and Wang, P. X., 2002. Architecture and evolution of the tide-dominated Changjiang (Yangtze) River Delta, China. *Sedimentary Geology*, **146** (3-4): 249-264.

Hu, D. X., Saito, Y., and Kempe, S., 1998. Sediment and nutrient transport to the coastal zone. In: *Asian Change in the Context of Global Climate Change: Impact of Natural and Anthropogenic Changes in Asia on Global Biogeochemical Cycles*. *IGBP Book Series 3*. Galloway, J. N., and Melillo, J. M., eds., Cambridge University Press, Cambridge, 245-270.

Hu, G., 2014. Sedimentation in the offshore area of Changjiang River Estuary and its responses to the environmental changes during the past century. PhD thesis. University of Chinese Academy of Sciences.

Hu, G., Li, A. C., Liu, J., Xu, G., Mei, X., and Kong, X. H., 2014. High resolution records of flood deposition in the mud area off the Changjiang River Mouth during the past century. *Chinese Journal of Oceanology and Limnology*, **32** (4): 909-920.

Huang, R. H., and Wu, Y. F., 1989. The influence of ENSO on the summer climate change in China and its mechanism. *Advance in Atmosphere Science*, **6**: 21-32.

Huang, H. J., Li, F., and Zhang, X. R., 2001. Water and sediment discharges from the Changjiang and Huanghe Rivers: A comparative study. In: *Land-Ocean Interaction in the Estuaries of the Changjiang and Pearl River and the Adjoining Re-*

gions. Hu, D. X., *et al*., eds., China Ocean Press, Beijing, 36-49.

Hulse, P., and Bentley, S. J., 2012. A ^{210}Pb sediment budget and granulometric record of sediment fluxes in a subarctic deltaic system: The Great Whale River, Canada. *Estuarine, Coastal and Shelf Science*, **109**: 41-52.

Li, T. G., Jiang, B., Sun, R. T., Zhang, D. Y., Liu, Z. X., and Li, Q., 2007. Evolution pattern of warm current system of eastern Yellow Sea since the last deglaciation. *Quaternary Science*, **27** (6): 945-954 (in Chinese with English abstract).

Li, Y. F., 1991. The development of the abandoned Yellow River Delta. *Geographical Research*, **10** (4): 29-39 (in Chinese with English abstract).

Lim, D. I., Choi, J. Y., Jung, H. S., Rho, K. C., and Ahn, K. S., 2007. Recent sediment accumulation and origin of shelf mud deposits in the Yellow and East China Seas. *Progress in Oceanography*, **73**: 145-159.

Lin, S. W., Hsieh, I. J., Huang, K. M., and Wang, C. H., 2002. Influence of the Yangtze River and grainsize on the spatial variations of heavy metals and organic carbon in the East China Sea continental shelf sediment. *Chemical Geology*, **182**: 377-394.

Liu, J., Li, S. Q., Wang, S. J., Yang, Z. G., Ge, Z. S., and Chang, J. H., 1999. Sea level changes of the Yellow Sea and formation of the Yellow Sea Warm Current since the last deglaciation. *Marine Geology & Quaternary Geology*, **19** (1): 13-24 (in Chinese with English abstract).

Liu, J., Saito, Y., Kong, X. H., Wang, H., and Zhao, L., 2009a. Geochemical characteristics of sediment as indicators of post-glacial environmental changes off the Shandong Peninsula in the Yellow Sea. *Continental Shelf Research*, **29**: 846-855.

Liu, J., Saito, Y., Kong, X. H., Wang, H., Wen, C., and Yang, Z. G., 2010. Sedimentary record of environmental evolution off the Yangtze River Estuary, East China Sea, during the last 13,000 years, with special reference to the influence of the Yellow River on the Yangtze River Delta during the last 600 years. *Quaternary Science Review*, **29**: 2424-2438.

Liu, J. P., Li, A. C., Xu, K. H., Veolzzi, D. M., Yang, Z. S., Milliman, J. D., and DeMaster, D. J., 2006. Sedimentary features of the Yangtze River-derived along-shelf clinoform deposit in the East China Sea. *Continental Shelf Research*, **26**: 2141-2156.

Liu, J. P., Xu, K. H., Li, A. C., Milliman, J. D., Velozzi, D. M., Xiao, S. B., and Yang, Z. S., 2007. Flux and fate of Yangtze River sediment delivered to the East China Sea. *Geomorphology*, **85**: 208-224.

Liu, J. P., Xue, Z., Ross, K., Wang, H. J., Yang, Z. S., Li, A. C., and Gao, S., 2009b. Fate of sediments delivered to the sea by Asian large rivers: Long-distance transport and formation of remote alongshore clinothems. *The Sedimentary Record*, **7** (4): 4-9.

Liu, M., and Fan, D. J., 2011. Geochemical records in the subaqueous Yangtze River Delta and their responses to human activities in the past 60 years. *Chinese Science Bulletin*, **56**: 552-561.

Liu, S. F., Shi, X. F., Liu, Y. G., Wu, Y. H., Yang, G., and Wang, X. C., 2013. Holocene paleoclimatic reconstruction based on mud deposits on the inner shelf of the East China Sea. *Journal of Asian Earth Science*, **69**: 113-120.

McLennan, S. M., 1993. Weathering and global denudation. *Journal of Geology*, **101** (2): 295-303.

Milliman, J. D., and Meade, R. H., 1983. World-wide delivery of river sediment to the oceans. *Journal of Geology*, **91**: 1-21.

Milliman, J. D., Beardsley, R. C., Yang, Z. S., and Limeburner, R., 1985a. Modern Huanghe-derived muds on the outer shelf of the East China Sea. *Continental Shelf Research*, **4**: 175-188.

Milliman, J. D., and Farnsworth, K. L., 2011. *River Discharge to the Coastal Ocean: A Global Synthesis*. Cambridge University Press, New York, 1-384.

Milliman, J. D., Shen, H. T., and Yang, Z. S., 1985b. Transport and deposition of river sediment in the Changjiang Estuary and adjacent shelf. *Continental Shelf Research*, **4**: 37-45.

Orpin, A. R., Carter, L., Page, M. J., Cochran, U. A., Trustrum, N. A., Gomez, B., Palmer, A. S., Mildenhall, D. C., Rogers, K. M., Brackley, H. L., and Northcote, L., 2010. Holocene sedimentary record from Lake Tutira: A template for upland watershed erosion proximal to the Waipaoa sedimentary system, northeastern New Zealand. *Marine Geology*, **270**: 11-29.

Pang, C. G., Li, K., and Hu, D. X., 2016. Net accumulation of suspended sediment and its seasonal variability dominated by shelf circulation in the Yellow and East China Seas. *Marine Geology*, **371**: 33-43.

Petley, D. N., 2010. The continental shelf and continental slope. In: *Sediment Cascades: An Integrated Approach*. Burt, T., and Allison, R., eds., Wiley-Blackwell, Chichester, 433-448.

Qiao, S. Q., Shi, X. F., Wang, G. Q., Zhou, L., Hu, B. Q., Hu, L. M., Yang, G., Liu, Y. G., Yao, Z. Q., and Liu, S. F., 2017. Sediment accumulation and budget in the Bohai Sea, Yellow Sea and East China Sea. *Marine Geology*, **390**: 270-281.

Qiao, S. Q., Yang, Z. S., and Liu, J. P., 2011. Records of late-Holocene East Asian winter monsoon in the East China Sea: Key grain-size component of quartz *versus* bulk sediments. *Quaternary International*, **230**: 106-114.

Ren, F. M., Yuan, Y., Sun, C. H., and Cao, L., 2012. Review of progress of ENSO studies in the past three decades. *Advances in Meteorology and Technology*, **2** (3): 17-24 (in Chinese with English abstract).

Stanley, D. J., and Chen, Z., 1993. Yangtze Delta, eastern China: 1: Geometry and subsidence of Holocene depocenter. *Marine Geology*, **112**: 1-11.

Sun, X. G., Fang, M., and Huang, W., 2000. Spatial and temporal variations in suspended particulate matter transport on the Yellow and East China Sea shelf. *Oceanologia et Limnologia Sinica*, **31** (6): 581-587.

Thamban, M., Rao, V. P., and Schneider, R. R., 2002. Reconstruction of late Quaternary monsoon oscillations based on clay mineral proxies using sediment cores from the western margin of India. *Marine Geology*, **186**: 527-539.

Thevenon, F., Guedron, S., Chiaradia, M., Loizeau, J. L., and Pote, J., 2011. Historic changes in natural and anthropogenic heavy metals deposition inferred from two contrasting Swiss Alpine lakes. *Quaternary Science Review*, **30**: 224-233.

Wang, S. W., and Gong, D. Y., 1999. ENSO events and their intensity during the past century. *Meteorological Monthly*, **25** (1): 9-14 (in Chinese with English abstract).

Wang, X., Shi, X. F., Liu, S. F., Wang, G. Q., Qiao, S. Q., Zhu, A. M., and Gao, J. J., 2012. High-resolution sedimentary record within a hundred years on the mud area near the Changjiang Estuary and discussion of its impacting factors. *Acta Sedimentologica Sinica*, **30** (1): 148-157 (in Chinese with English abstract).

Wang, Z. H., Saito, Y., Hori, K., and Chen, Z. Y., 2005. Yangtze offshore, China: Highly laminated sediments from the transition zone between subaqueous delta and the continental shelf. *Estuary Coast and Shelf Science*, **62** (1-2): 161-168.

Xia, N., Zhang, Q., Yao, D., and Li, G. H., 2008. Geochemical analysis of marine sediments using fused glass disc by X-ray fluorescence spectrometry. *Chinese Journal of Oceanology and Limnology*, **26** (4): 475-479.

Xiao, S. B., Li, A. C., Jiang, F. Q., Li, T. G., Huang, P., and Xu,

Z. K., 2004. Sedimentary records and its climatic implications of mud along the Min-Zhe Coast since 2 ka BP. *Chinese Science Bulletin*, **49** (21): 2233-2238 (in Chinese with English abstract).
Xiao, S. B., Li, A. C., Jiang, F. Q., You, Z., and Chen, L., 2005. Provenance analysis of mud along the Min-Zhe Coast since 2 ka BP. *Acta Sedimentologica Sinica*, **23** (2): 268-274 (in Chinese with English abstract).
Xiao, S. B., Li, A. C., Liu, W. G., Zhao, J. C., and Xu, F. J., 2009. Provenance analysis of muddy sediments along the Min-Zhe Coast. *Progress in Natural Science*, **19** (2): 185-191 (in Chinese with English abstract).
Xiang, R., Yang, Z. S., Saito, Y., Fan, D. J., Chen, M. H., Guo, Z. G., and Chen, Z., 2008. Paleoenvironmental changes during the last 8400 years in the southern Yellow Sea: Benthic foraminiferal and stable isotopic evidence. *Marine Micropaleontology*, **67**: 104-119.
Yang, X. Q., Zhu, Y. M., Xie, Q., Ren, X. J., and Xu, G. Y., 2004. Advances in studies of Pacific Decadal Oscillation. *Chinese Journal of Atmospheric Sciences*, **28** (6): 979-992 (in Chinese with English abstract).
Yang, Z. S., and Chen, X. H., 2007. Centurial high resolution records of sediment grain-size variation in the mud area off the Changjiang (the Yangtze River) Estuary and its influential factors. *Quaternary Science*, **27** (5): 690-699.
Yang, Z. S., Lei, K., and Guo, Z. G., 2007. Effect of a winter storm sediment transport and resuspension in the distal mud area, the East China Sea. *Journal of Coastal Research*, **23** (2): 310-318.
Ye, Q. C., 1986. On the development of the abandoned Yellow River Delta in northern Jiangsu Province. *Acta Geographica Sinica*, **41** (2): 112-122 (in Chinese with English abstract).
Yu, K. F., Zhao, J. X., Shi, Q., Chen, T. G., Wang, P. X., Collerson, K. D., and Liu, T. S., 2006. U-series dating of dead Porites corals in the South China Sea: Evidence for episodic coral mortality over the past two centuries. *Quaternary Geochronology*, **1**: 129-141.
Yu, Z. Y., Chen, D. C., and Jin, L., 1986. The formation and erosion of the old Huanghe River submarine delta in the northern part of Jiangsu beach. *Acta Oceanologica Sinica*, **8** (2): 197-206 (in Chinese with English abstract).
Zhang, R. S., 1984. Land-forming history of the Huanghe River Delta and coastal plain of northern Jiangsu. *Acta Geographica Sinica*, **39** (2): 173-184 (in Chinese with English abstract).
Zhao, Y. Y., and Yan, M. C., 1994. *Geochemistry of Sediments in Chinese Shallow Sea*. Science Press, Beijing, 1-174.
Zhou, L. T., Tam, C. Y., Zhou, W., and Chan, J. C. L., 2009. Influence of South China Sea SST and the ENSO on winter rainfall over South China. *Advances in Atmosphere Science*, **27**: 832-844.

(Edited by Chen Wenwen)